Micro-differential boundary conditions modelling the absorption of acoustic waves by 2D arbitrarily-shaped convex surfaces

Hélène Barucq, Julien Diaz, Véronique Duprat

Commun. Comput. Phys.
doi: 10.4208/cicp.311209.260411s

Vol. **11**, No. 2, pp. 674-690
February 2012

Micro-Differential Boundary Conditions Modelling the Absorption of Acoustic Waves by 2D Arbitrarily-Shaped Convex Surfaces

Hélène Barucq[1,2], Julien Diaz[1,2] and Véronique Duprat[2,1,*]

[1] *INRIA Bordeaux-Sud Ouest, Team-project MAGIQUE-3D.*
[2] *LMA, CNRS UMR 5142, University of Pau, France.*

Received 31 December 2009; Accepted (in revised version) 26 April 2011

Available online 24 October 2011

Abstract. We propose a new Absorbing Boundary Condition (ABC) for the acoustic wave equation which is derived from a micro-local diagonalization process formerly defined by M.E. Taylor and which does not depend on the geometry of the surface bearing the ABC. By considering the principal symbol of the wave equation both in the hyperbolic and the elliptic regions, we show that a second-order ABC can be constructed as the combination of an existing first-order ABC and a Fourier-Robin condition. We compare the new ABC with other ABCs and we show that it performs well in simple configurations and that it improves the accuracy of the numerical solution without increasing the computational burden.

AMS subject classifications: 35L05

Key words: Wave equation, micro-local diagonalization, absorbing boundary condition, finite element formulation.

1 Introduction

The numerical simulation of waves propagation generally involves boundary conditions which both represent the behavior of waves at infinity and provide a mathematical tool to define a bounded computational domain in which a finite element method can be applied. Most of these conditions can be justified as an approximation of the Dirichlet-to-Neumann operator and when they both preserve the sparsity of the finite element matrix and enforce dissipation into the system, they are called Absorbing Boundary Conditions (ABC). Obviously an ABC impacts the accuracy of the numerical solution which can be improved by using high-order conditions. Nevertheless a high-order condition

*Corresponding author. *Email addresses:* helene.barucq@inria.fr (H. Barucq), julien.diaz@inria.fr (J. Diaz), veronique.duprat@univ-pau.fr (V. Duprat)

requires to introduce auxiliary unknowns to be easily employed in a finite element formulation [12–14] which increases the computational cost significantly. Moreover, increasing the order of the condition can destroy the long-time stability of the wave equation. Another limitation of existing ABCs is the type of surface bearing the ABC. Most of the high-order ABCs have been derived for flat surfaces. They can be used for more general boundaries which can be described by a collection of segments. Nevertheless, it is necessary to introduce matching conditions between each segments which can be cumbersome to implement.

In this paper, we show how to construct an ABC that fits the following criteria:

1. the ABC can be apply to arbitrarily-shaped boundaries;
2. the ABC does not require significant additional computations to be handled in a finite element formulation;
3. the ABC preserves the long-time stability of the wave equation.

For that purpose, we investigate the possibility of improving an existing first-order ABC which can be applied on arbitrarily-shaped boundaries. To minimize the computational cost, we limit our study to the construction of second-order differential conditions. Regardless of the implementation aspect, we can also note that Engquist and Majda showed that conditions of order greater than two could lead to an ill-posed problem. The existing condition that we use is the first-order condition involving the curvature of the absorbing boundary [10]. This condition is very easy to include in a variational formulation. To justify our choice, we begin with comparing the curvature condition with the BGT2 condition, introduced by Bayliss, Gunzburger and Turkel in [5], extended to the time domain, knowing that the BGT2 condition is widely used by engineers. We show that the extended BGT2 condition requires to introduce an auxiliary unknown and that it performs as well as the curvature condition. We then investigate how to improve the performances of the curvature condition. For that purpose, we use a generalization of the Taylor diagonalization process by considering the principal symbol of the wave equation both in the hyperbolic and the elliptic regions. Our approach meets an idea that was formerly investigated in [12–14] but for flat surfaces extending conditions formerly proposed by Higdon [15]. By using a classical finite element scheme, Hagstrom *et al.* [12–14] have shown the improvements induced by the new condition. Nevertheless, we have observed that the Hagstrom *et al.* condition is unstable when employed in an Interior Penalty Discontinuous Galerkin (IPDG) formulation while our new condition seems to be stable. Moreover, the Hagstrom *et al.* condition seems to be difficult to use on curved surfaces while our condition can be applied straightforwardly, without any corner condition. The new condition that we construct is the combination of two boundary conditions which each leads to a long-time stable system. Hence the new ABC should outperform the Hagstrom *et al.* condition.

In this paper, we consider a model problem for the time-dependent wave equation in a two-dimensional domain Ω with an obstacle inside and an ABC on its external bound-

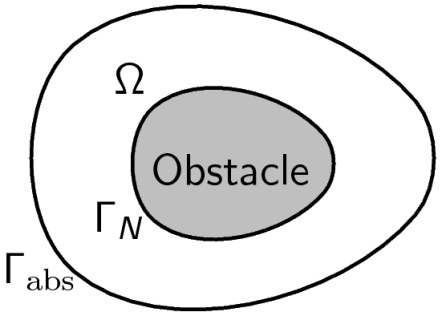

Figure 1: Studied domain.

ary (see Fig. 1). We have

$$(\mathcal{S})\begin{cases}\partial_t^2 u-\operatorname{div}\left(c^2\nabla u\right)=f, & \text{in } (0,T)\times\Omega,\\ u(0,x)=0\,; \quad \partial_t u(0,x)=0, & \text{in } \Omega,\\ \partial_{\mathbf{n}} u=0, & \text{on } \Gamma_N,\\ \partial_{\mathbf{n}} u=Bu, & \text{on } \Gamma_{\text{abs}},\end{cases}$$

where f is the source function, c the velocity of the wave u (the unknown field), T the final time, $\mathbf{n}$ the unit outward normal vector, Γ_N and Γ_{abs} respectively the boundary with the Neumann condition and the ABC which is represented by the operator B. The operator B is differential, for instance, it reads $\frac{1}{c}\partial_t$ which corresponds to the simplest ABC.

In this paper, we restrict our study to the 2D case but the extension to the 3D case is relatively unmediated.

2 The time domain BGT2 condition

We aim at constructing efficient ABCs of order 2 which can be used for the acoustic wave equation on arbitrarily-shaped boundaries. The most straightforward approach consists in considering a second-order ABC that can be derived easily from the BGT2 condition. Indeed this condition is widely used by engineers for the Helmholtz equation because of its efficiency and its simplicity of implementation.Then it could perform well in the time domain too. We restrict our study to the case of a circular boundary but the same work can be done for an ellipse by using the condition proposed in [17].

In the time harmonic domain, the BGT-2 ABC is given by

$$\partial_n u=\left(ik-\frac{1}{2R}+\frac{1}{8R(1-ikR)}\right)u+\frac{1}{2R(1-ikR)}\partial_\theta^2 u, \tag{2.1}$$

where θ is the angular polar coordinate, R is the radius of the circle and k denotes the frequency.

To write the condition in the time-domain, we apply an inverse Fourier transform to (2.1). We then get

$$\partial_n u+\partial_t u+\frac{1}{2R}u=(1+R\partial_t)^{-1}\left(\frac{1}{8R}u+\frac{1}{2R}\partial_\theta^2 u\right). \tag{2.2}$$

The resulting condition is nonlocal since it involves the inverse of $1+R\partial_t$ but it can be easily localized by introducing an auxiliary variable as follows

$$\begin{cases} \partial_n u+\partial_t u+\dfrac{1}{2R}u=w, \\ (1+R\partial_t)w=\dfrac{1}{8R}u+\dfrac{1}{2R}\partial_\theta^2 u. \end{cases} \tag{2.3}$$

Written as above, the ABC corresponds to a perturbation of the curvature ABC (C-ABC) defined by

$$\partial_t u+\partial_n u+\frac{1}{2R}u=0,$$

and which has been derived by several authors (see for instance Engquist and Majda [10]) by applying different approaches. In the following, the condition (2.3) will be called TD-BGT2 ABC. To measure how the new condition performs, we have included it in a IPDG formulation [11] of the wave equation. We refer the reader to the appendix A for more detail on the IPDG formulation. This leads to the solution of the algebraic system

$$\begin{cases} M\dfrac{d^2\mathbf{U}}{dt^2}+B\dfrac{d\mathbf{U}}{dt}+B_\kappa\mathbf{U}+K\mathbf{U}-G\mathbf{W}=F, \\ C\mathbf{W}+RC\dfrac{d\mathbf{W}}{dt}=\dfrac{D}{8R}\mathbf{U}-\dfrac{E}{2R}\mathbf{U}, \end{cases} \tag{2.4}$$

where $\mathbf{U}$ and $\mathbf{W}$ are the unknowns, F the source vector, M, B, B_κ, C, D and G block-diagonal mass matrices and K, E are stiffness matrices. Except for M and K, all these matrices are only defined on Γ_{abs}. The system reduces to the first algebraic equation when the C-ABC is used, that is with $G=0$.

For the time discretization, we use the classical second-order Leap-Frog scheme, which is quasi-explicit since all the matrices are block-diagonal and therefore easily invertible.

We have compared the performances of the TD-BGT2 conditions to the ones of the C-ABC for two simple configurations. In the first configuration, the domain Ω is a disk of radius 3m, centered in $(0\text{m}, 0\text{m})$ and Γ_{abs} is the boundary of Ω (see Fig. 1). We consider zero initial condition and an off-center point source in space at $(0\text{m}, 1\text{m})$ which is a second-derivative of a Gaussian with a dominant frequency of 1Hz.

In the second configuration, the domain Ω is a ring centered in $(0\text{m}, 0\text{m})$ of internal radius 1m and of external radius 3m. Γ_{abs} is the external boundary of the ring and Γ_N is the internal one (see Fig. 2). We consider zero initial conditions and an off-center point source in space at $(0\text{m}, 1.5\text{m})$ which is a second-derivative of a Gaussian with a dominant frequency of 1Hz.

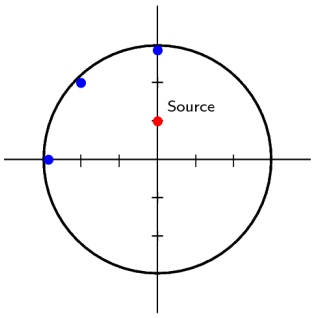

Figure 2: Computational domain: Circle.

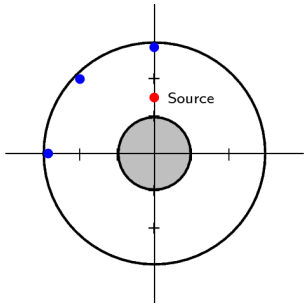

Figure 3: Computational domain: Ring.

In both configurations, we set the final time $T=40$s.

To compare the efficiency of the TD-BGT2 condition to the one of the C-ABC, we set three receivers near the absorbing boundary at points $(0\text{m}, 2.85\text{m})$, $(-2\text{m}, 2\text{m})$ and $(-2.85\text{m}, 0\text{m})$ and we compute the relative $L^2_{(x,y)}([0,T])$ error at each receiver which coordinates are (x,y). This error is defined by

$$\frac{\left(\int_0^T (u_{app}(t,(x,y))-u_{ex}(t,(x,y)))^2 dt\right)^{1/2}}{\left(\int_0^T (u_{ex}(t,(x,y)))^2 dt\right)^{1/2}},$$

where u_{app} is the approximation of the solution and u_{ex} is the exact solution obtained thanks to a Cagniard-de Hoop method [7]. The error is given after 6000 iterations (with a time step equal to $6.959e-3$s). In Table 1, we give the results for the first configuration and in Table 2, the ones for the second one. Each column corresponds to a receiver and each line to a given ABC. We can remark that the TD-BGT2 condition gives better results than the C-ABC. This is not surprising since it corresponds to a second-order approximation of the Dirichlet-to-Neumann operator while the C-ABC is a first-order approximation. The first column depicts very good results for both conditions because the corresponding receiver is set at normal incidence and we already know that the C-ABC is very efficient in this case.

Table 1: Relative L^2 error (in %) – circle.

	(0, 2.85)	(-2, 2)	(-2.85, 0)
C-ABC	1.136	2.347	3.154
TD-BGT2	1.059	2.182	2.939

Table 2: Relative L^2 error (in %) – ring.

	(0, 2.85)	(-2, 2)	(-2.85, 0)
C-ABC	1.42	7.21	5.77
TD-BGT2	1.30	6.71	5.39

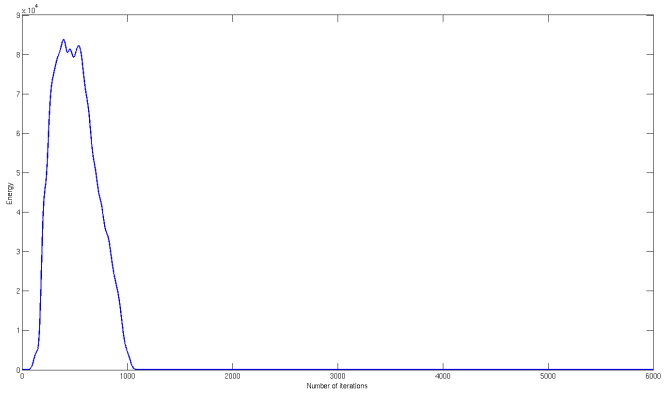

Figure 4: Decay of the energy: TD-BGT2 ABC.

Even if we have not been able to prove the decay of an energy, we have computed the classical one $E^{n+1/2}$ given by

$$E^{n+1/2}=\left(M\frac{U^{n+1}-U^{n-1}}{\Delta t},\frac{U^{n+1}-U^{n-1}}{\Delta t}\right)+\left(KU^n,U^{n+1}\right), \tag{2.5}$$

where $U^n=\mathbf{U}(n\Delta t)$ to show the stability of the method. We have plotted in Fig. 4 the evolution of this energy with respect to the number of iterations in time until 6000 iterations. We can see that the scheme remains stable. We precise that we have performed this experiment until 1000000 iterations (6959s) and we have not observe any instability. We thus claim that the TD-BGT2 preserves the long-time stability of the wave equation.

Hence the TD-BGT2 ABC outperforms the C-ABC but the improvement is not significant enough considering that we have added an auxiliary function to apply the TD-BGT2 ABC and we have thus increased the computational burden. Moreover, the BGT2-ABC can not be applied on any arbitrarily-shaped boundary, even if it can be written easily for an ellipse [17]. Hence the TD-BGT2 ABC does not satisfy all the criteria defined in the introduction.

3 A new family of second-order ABCs for the acoustic wave equation

In this section, we are interested in constructing a new absorbing boundary condition using the micro-diagonalization method developed by M.E. Taylor [18]. We want this condition to be written for all regular convex domains and to take into account both propagating and evanescent waves. Indeed, our idea is to compose two first-order conditions: one for the propagating waves and the other one for the evanescent waves. First, we present the main steps of this micro-diagonalization method. For the sake of simplicity, the velocity c is supposed to be equal to 1m.s^{-1}.

3.1 The micro-diagonalization method applied to the wave equation

In this section, we tackle the enrichment of existing ABCs by applying the factorization theorem initially established by M.E. Taylor [18] to study the propagation of singularities of strictly hyperbolic systems. We consider two different approaches and we analyze the impact of the modified condition on the accuracy of the numerical solution. Just as was previously mentioned, we would like to investigate the possibility of constructing high-order absorbing boundary conditions without involving high-order differential operators. Hence we limit our work to the application of the first step of factorization which means that we are only dealing with the diagonalization of the principal symbol of the wave equation. Indeed, according to [2], the following steps necessarily involve differential operators with order higher than two.

The ABCs that we consider are derived from the micro-local approximation of the Dirichlet-to-Neumann operator related to the artificial surface Γ_{abs}. We thus begin with rewriting the acoustic wave equation in a local coordinate system (r,s). The couple (r,s) describes a point in the neighborhood of Γ_{abs} in such a way that $\Gamma_{\text{abs}}=\{r=0\}$. We use the same coordinate system as in [3] and the acoustic wave equation reads then as

$$\partial_t^2 u-\partial_r^2 u-\kappa_r\partial_r u-h^{-1}\partial_s\left(h^{-1}\partial_s u\right)=0, \tag{3.1}$$

where κ is the curvature of Γ_{abs}, $h=1+r\kappa(s)$ and $\kappa_r=h^{-1}\kappa$.

Next, to apply Taylor's method, we rewrite (3.1) as a first-order system. We thus introduce an auxiliary unknown v which satisfies $\partial_t v+\partial_r u=0$ in a neighborhood of Γ_{abs} and if $\mathbf{U}$ denotes the field $\mathbf{U}=(v,u)$, $\mathbf{U}$ is solution to the first-order system

$$\partial_r\mathbf{U}=L\mathbf{U}.$$

The entries of L are first-order pseudodifferential operators and $\sigma(L)=\mathcal{L}=\mathcal{L}_1+\mathcal{L}_0$ is given by

$$\mathcal{L}_1=\begin{pmatrix} 0 & -\dfrac{h^{-2}\xi^2-\omega^2}{i\omega} \\ -i\omega & 0 \end{pmatrix}\in S^1 \quad \text{and} \quad \mathcal{L}_0=\begin{pmatrix} -\kappa_r & -\dfrac{h^{-3}\partial_s(h)\xi}{\omega} \\ 0 & 0 \end{pmatrix}\in S^0,$$

where ξ and ω are the dual variables associated respectively to s and t. We use standard notations such as $\sigma(L)$ for the symbol of L and we refer the reader to [16] for the definition of spaces S^m. Let λ_1 denote the symbol $\lambda_1=\left(h^{-2}\xi^2-\omega^2\right)^{1/2}$. Then, when $\lambda_1\neq 0$, the principal symbol of $\mathcal{L}$ admits two single eigenvalues λ_1 and $-\lambda_1$. When $h^{-2}\xi^2-\omega^2>0$, λ_1 is real and when $h^{-2}\xi^2-\omega^2<0$, λ_1 is imaginary. Following [2,9,10], we introduce

$$\mathcal{V}_0=\frac{1}{\sqrt{2}}\begin{pmatrix} \dfrac{i\omega}{\lambda_1} & 1 \\ 1 & -\dfrac{\lambda_1}{i\omega} \end{pmatrix} \tag{3.2}$$

and then we have

$$\mathcal{V}_0\mathcal{L}_1\mathcal{V}_0^{-1}=\begin{pmatrix}\lambda_1 & 0\\ 0 & -\lambda_1\end{pmatrix}. \tag{3.3}$$

Now, a first-order ABC can be derived from the approximation and the localization of the global boundary condition

$$((I+K_{-1})\,V_0\mathbf{U})_2=0 \quad \text{on } \Gamma_{\text{abs}}, \tag{3.4}$$

where K_{-1} is a regularizing operator which principal symbol $\mathcal{K}_{-1}$ is given by

$$\mathcal{K}_{-1}=\begin{pmatrix}0 & -\dfrac{i\kappa\omega^3}{4\lambda_1^4}\\ -\dfrac{i\kappa\omega}{4\lambda_1^2} & 0\end{pmatrix}. \tag{3.5}$$

Remark 3.1. When $h^{-2}\xi^2-\omega^2>0$, the frequencies (ω,ξ) cover the elliptic region. If not, (ω,ξ) lie in the hyperbolic region.

When λ_1 is imaginary, (3.4) can be rewritten as, after using a truncated Taylor expansion on λ_1 under a high-frequency hypothesis: $\omega^2\gg h^{-2}\xi^2$,

$$\partial_t u+\partial_n u+\frac{\kappa}{2}u=0 \quad \text{on } \Gamma_{\text{abs}}, \tag{3.6}$$

which is the C-ABC presented in the previous section in the case of a circle. The resulting condition involves differential operators but it should be called micro-differential since it is justified in the propagating cone $\omega^2\gg h^{-2}\xi^2$.

The technique of diagonalization wave equation with variable coefficients has been used by Engquist and Majda [10] to construct absorbing boundary conditions but it was applied only when the operator $\mathcal{K}_{-1}$ is anti-diagonal. That $\mathcal{K}_{-1}$ is anti-diagonal is sufficient to diagonalize the principal symbol of the wave equation and therefore construct absorbing boundary conditions. However the matrix $\mathcal{K}_{-1}$ is actually not unique because its diagonal coefficients are not fixed by the diagonalization process. Here we have chosen zero but we could have used any functions in S^{-1}.

In our work, we first consider the case where the operator $\mathcal{K}_{-1}$ has a nonzero diagonal entry, which determines a family of boundary conditions depending on a parameter. This is the object of Section 3.2. The non-diagonal term is fixed to be consistent with the symbols of degree -1. It is interesting to note that in doing exactly the same calculations as in the work of Engquist and Majda, we obtain conditions which localization of lowest degree, ie the differential operator obtained from a Taylor approximation of order 1, will be necessarily a differential operator of order two. In Section 3.3, we adapt the technique of Engquist and Majda to the elliptic region.

3.2 Improving the C-ABC in the hyperbolic region

As it was previously announced, a first task consists in considering the family of ABCs that can be derived when $\mathcal{K}_{-1}$ is modified by introducing a non-zero diagonal term. This idea has been formally applied in [4] for the 2D Maxwell system but only from a theoretical point of view. To the best of our knowledge, the numerical impact of this approach has never been investigated. Herein, we propose to modify $\mathcal{K}_{-1}$ as follows

$$\mathcal{K}_{-1}=\begin{pmatrix} 0 & -\dfrac{i\kappa\omega^3}{4\lambda_1^4} \\ -\dfrac{i\kappa\omega}{4\lambda_1^2} & \dfrac{\gamma(s)}{\lambda_1} \end{pmatrix}, \tag{3.7}$$

where γ is a parameter depending only on the curvilinear abscissa s. The other diagonal term is kept equal to zero because it is not involved in writing the boundary condition. Indeed, it affects only the part of the reentrant wave field that should not be modeled. We then get

Theorem 3.1. *A family of first-order condition depending on a parameter is*

$$\partial_t(\partial_n u+\partial_t u)=\Big(\frac{\kappa}{4}-\gamma\Big)\partial_n u-\Big(\frac{\kappa}{4}+\gamma\Big)\partial_t u \quad \text{on } \Gamma_{abs}. \tag{3.8}$$

Proof. We recall that the first-order boundary condition is given by

$$((I+K_{-1})V_0\mathbf{U})_2=0 \quad \text{on } \Gamma_{\text{abs}}. \tag{3.9}$$

The symbol of the corresponding operator reads as

$$\sigma((I+K_{-1})V_0)=((\mathcal{I}_2+\mathcal{K}_{-1})\mathcal{V}_0)+\mathcal{R}_{-2},$$

where $\mathcal{R}_{-2}\in S^{-2}$. Therefore, the truncation of $\sigma((I+K_{-1})V_0)$ in S^{-1} is given by

$$\begin{aligned}\tau_{-1}((I+K_{-1})V_0)&=((\mathcal{I}_2+\mathcal{K}_{-1})\mathcal{V}_0)\\ &=\frac{1}{\sqrt{2}}\begin{pmatrix} \dfrac{i\omega}{\lambda_1}-\dfrac{i\kappa\omega^3}{4\lambda_1^4} & 1+\dfrac{\kappa\omega^2}{4\lambda_1^3} \\ \dfrac{\kappa\omega^2}{4\lambda_1^3}+1+\dfrac{\gamma(s)}{\lambda_1} & -\dfrac{i\kappa\omega}{4\lambda_1^2}-\dfrac{\lambda_1}{i\omega}-\dfrac{\gamma(s)}{i\omega} \end{pmatrix}.\end{aligned} \tag{3.10}$$

Using a first-order Taylor expansion for $\omega>>h^{-1}\xi$, we then obtain

$$\tau_{-1}((\mathcal{I}_2+\mathcal{K}_{-1})\mathcal{V}_0)_1=\frac{1}{\sqrt{2}}\begin{pmatrix} 1-\dfrac{i\kappa}{4\omega} & 1+\dfrac{i\kappa}{4\omega} \\ 1+\dfrac{i\kappa}{4\omega}+\dfrac{\gamma}{i\omega} & \dfrac{i\kappa}{4\omega}-1-\dfrac{\gamma}{i\omega} \end{pmatrix}. \tag{3.11}$$

Then, combining (3.4) with the definition of **U**, we get

$$\partial_t(\partial_n u+\partial_t u)=\left(\frac{\kappa}{4}-\gamma\right)\partial_n u-\left(\frac{\kappa}{4}+\gamma\right)\partial_t u \quad \text{on } \Gamma_{\text{abs}}.$$

This completes the proof. □

We then get a second-order condition depending on a parameter γ. When $\gamma=0$, we can recover the C-condition by simplifying the Taylor expansion.

3.3 Diagonalization in the elliptic region

The matrix $\mathcal{K}_{-1}$ can be defined when (ω,ξ) covers the elliptic region exactly in the same way than in Section 3.2. We get

Theorem 3.2. *A first-order condition taking into account the evanescent waves is given by*

$$\partial_n u+\beta u=0 \quad \text{on } \Gamma_{abs}. \tag{3.12}$$

Proof. We proceed in the same way as in the proof of Theorem 3.1. Now, $\lambda_1=\sqrt{h^{-2}\xi^2-\omega^2}$ is real and as in [13], we propose to apply the parametrization $\lambda_1=\beta$, with $\beta>0$. We then get

$$\tau_{-1}((\mathcal{I}_2+\mathcal{K}_{-1})\mathcal{V}_0)=\frac{1}{\sqrt{2}}\begin{pmatrix}\frac{i\omega}{\beta} & 1\\ 1 & -\frac{\beta}{i\omega}\end{pmatrix}$$

and the resulting condition reads as

$$\partial_n u+\beta u=0 \quad \text{on } \Gamma_{\text{abs}}.$$

This completes the proof. □

We have then a Fourier-Robin condition which has been derived from the approximation of the Dirichlet-to-Neumann operator into the elliptic region. We can observe that if the wave equation is coupled with (3.12) only, the resulting system is conservative when $\beta>0$. Indeed, if $\mathcal{E}(t)$ denotes the functional

$$\mathcal{E}(t)=\frac{1}{2}\int_\Omega\left(|\partial_t u|^2+|\nabla u|^2\right)dx+\frac{1}{2}\int_{\Gamma_{\text{abs}}}\beta|u|^2dF,$$

defined for any regular solution to the wave equation, $t\longmapsto\mathcal{E}(t)$ is a constant and it defines an energy if $\beta>0$.

3.4 A new family of ABCs

We are now willing to derive a new family of ABCs. The construction is straightforward since it is based on the combination of the conditions (3.6) and (3.12). The idea of combining both the propagating and the evanescent conditions follows the representation of the wave field U from its inverse Fourier transform that can be defined from the algebraic relation involving $\mathcal{L}$. Indeed, the inverse Fourier transform is used to represent the wavefield as the sum of two integrals which are defined respectively in the cone of propagation and the elliptical region. By construction, each integral satisfies the exact condition making the approximate condition. Since both approximate conditions commute, an approximation of the exact condition is obtained by combining the two approximate conditions. The idea of decomposing the wave field will be included explicitly in the next section devoted to numerical experiments.

Proposition 3.1. A second-order family of ABCs taking both propagating and evanescent waves into account reads as

$$(\partial_n+\beta)\left(\partial_t+\partial_n+\frac{\kappa}{2}\right)u=0 \quad \text{on } \Gamma_{\text{abs}}. \tag{3.13}$$

We could have considered the combination of the Fourier-Robin condition with the one-parameter family of conditions but we would have obtained a third-order family of conditions. Moreover, we are going to show that there is numerically no interest to apply the one-parameter condition as compared to the C-ABC.

4 Numerical results

In this section, we first investigate the performances of the ABC (3.8) for different values of γ. We conclude that $\gamma=0$ is the optimal value, which justifies the definition of the ABC (3.13). Then, we compare the accuracy of the ABC (3.13) to the ones of the C-ABC and of the TD-BGT2 ABC.

4.1 Numerical study of the one-parameter family of conditions

Let us consider the implementation of the ABC (3.8) into a finite element formulation. We propose to define an auxiliary unknown to obtain an ABC easier to introduce in the formulation. The ABC (3.8) is rewritten as follows:

$$\partial_n u=-\partial_t u-\frac{\kappa}{2}\left(\partial_t-\frac{\kappa}{4}+\gamma\right)^{-1}\partial_t u \quad \text{on } \Gamma_{\text{abs}}$$

and we define ψ as the surface field satisfying

$$\left(\partial_t-\frac{\kappa}{4}+\gamma\right)\psi=\partial_t u \quad \text{on } \Gamma_{\text{abs}}.$$

Table 3: Relative L^2 error (in %) – circle.

	(0, 2.85)	(-2, 2)	(-2.85, 0)
C-ABC	1.136	2.347	3.154
$\gamma=\kappa$	1.138	2.460	3.283
$\gamma=\kappa/3$	1.131	2.358	3.168
$\gamma=3\kappa$	1.353	2.782	3.596

Then the solution u satisfies

$$\partial_n u+\partial_t u=-\frac{\kappa}{2}\psi \quad \text{on } \Gamma_{\text{abs}},$$

which can be easily included into the variational formulation (see Appendix A). We have tested the ABC (3.8) for different values of the parameter γ in the case of the disk without obstacle described at Section 2. In Table 3, we provide the relative L^2 error at each receiver for $\gamma=\kappa$, $\kappa/3$ and 3κ. We can easily see that the impact of the parameter γ is not significant. Hence, in the following, we will consider the C-ABC for the propagating waves which gives similar results than the ABC (3.8) but with a smaller computational cost since there is no need to introduce an auxiliary function.

4.2 Numerical study of the new ABC

To implement the ABC (3.13) into a finite element formulation, we propose to use a more convenient expression of (3.13) which can be easily introduced into the variational formulation thanks to an auxiliary unknown. The ABC (3.13) is rewritten as

$$\partial_n u=-\partial_t u-\frac{\kappa}{2}u+\left(\beta+\partial_t-\frac{\kappa}{2}\right)^{-1}\left(\partial_s^2-\frac{\kappa^2}{4}\right)u \quad \text{on } \Gamma_{\text{abs}}$$

and we define ψ as the surface field satisfying

$$\left(\beta+\partial_t-\frac{\kappa}{2}\right)\psi=\left(\partial_s^2-\frac{\kappa^2}{4}\right)u \quad \text{on } \Gamma_{\text{abs}}.$$

Then the solution u satisfies

$$\partial_n u+\partial_t u+\frac{\kappa}{2}u=\psi \quad \text{on } \Gamma_{\text{abs}}.$$

Remark 4.1. As for the TD-BGT2 ABC, this condition can be seen as a penalization of the first-order C-ABC. This is not surprising because the condition is the combination of the curvature condition with a Robin condition. Moreover, this writing expresses explicitly that the wave field u is not only propagating and the correction is represented by ψ.

After having applied an IPDG space discretization, the algebraic form of the problem is given by

$$\begin{cases} M\dfrac{d^2\mathbf{U}}{dt^2}+B\dfrac{d\mathbf{U}}{dt}+B_\kappa\mathbf{U}+K\mathbf{U}-G\mathbf{\Psi}=F, \\ \beta C\mathbf{\Psi}+C\dfrac{d\mathbf{\Psi}}{dt}-C_\kappa\mathbf{\Psi}=-\dfrac{D_{\kappa^2}}{4}\mathbf{U}-E\mathbf{U}, \end{cases} \tag{4.1}$$

where the mass-matrices M, B, B_κ, G, C, C_κ and D_{κ^2} are block-diagonal.

Remark 4.2. As in the case of the TD-BGT2 ABC, the matrices B, B_κ, G, C, C_κ, D_{κ^2} and E are not defined outside of the boundary, so the system to solve inside the domain is the same as in the case when $\Gamma_{\text{abs}}=\varnothing$.

As for the TD-BGT2 ABC, we use a second-order Leap-Frog scheme for the time discretization.

To evaluate the efficiency of our condition, we compare it with the TD-BGT2 ABC and the C-ABC in the two configurations described at Section 2. In Fig. 5 (resp. Fig. 6) we represent the relative L^2 error computed at receiver $(-2\text{m}, 2\text{m})$ for various values of β between 0.3 and 5 in the first (resp. second) configuration. These figures indicate that the optimal value of β is about 0.7 for the two configurations. We have obtained similar results for the receivers at point $(0\text{m}, 2.85\text{m})$ and $(-2.85\text{m}, 0\text{m})$. In Table 4 (resp. Table 5), we compare the relative L^2 error obtained for $\beta=0.7$ to the ones obtained with a C-ABC and a TD-BGT2 ABC in the first (resp. second) configuration.

Let us mention that the optimal value of β depends on many parameters. For instance, it depends on the curvature of the boundary and on the space step h. We have reproduced the experiment on a finer grid and we have obtained an optimal value of 2.7. It seems that the value of β is inversely proportional to a power of h (maybe h^2). We find a behavior that is similar to that analyzed by Dolean et al. [8] in the case of optimized transmission conditions.

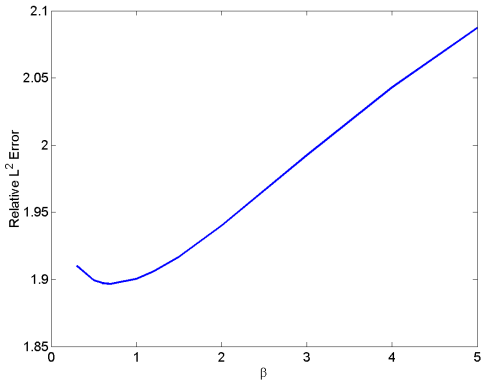

Figure 5: Relative L^2 error (in %) at point $(-2\text{m}, 2\text{m})$: Circle.

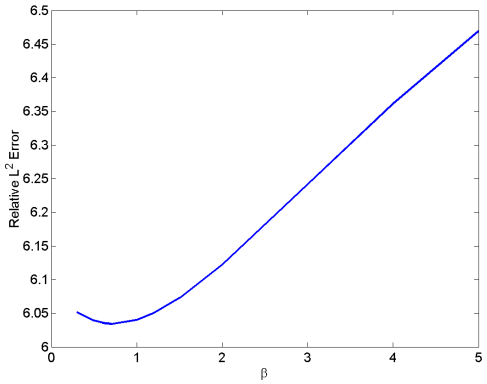

Figure 6: Relative L^2 error (in %) at point $(-2\text{m}, 2\text{m})$: Ring.

Table 4: Relative L^2 error (in %) – circle.

	(0, 2.85)	(-2, 2)	(-2.85, 0)
curvature	1.14	2.35	3.15
BGT-2	1.06	2.18	2.94
$\beta = 0.7$	1.01	1.90	2.59

Table 5: Relative L^2 error (in %) – ring.

	(0, 2.85)	(-2, 2)	(-2.85, 0)
curvature	1.42	7.21	5.77
BGT-2	1.30	6.71	5.39
$\beta = 0.7$	1.22	6.03	4.84

As we already observed in the previous experiments, the solution at the first receiver located above the source is very accurate, whatever the condition is. This is due to the fact that most of the waves impact the boundary at normal incidence above the source. On the contrary, the solutions obtained at the two other receivers are more accurate with the new condition than with the C-ABC or the TD-BGT2 ABC.

As for the TD-BGT2 ABC, we have not been able to prove the decay of an energy and so we have computed the energy defined in (2.5). We have plotted in Fig. 7 the evolution of this energy with respect to the number of iterations in time until 6000 iterations. We can see that the scheme remains stable. We precise that we have performed this experiment until 1000000 iterations (6959s) and we have not observe any instability. We thus claim that the new condition preserves the long-time stability of the wave equation.

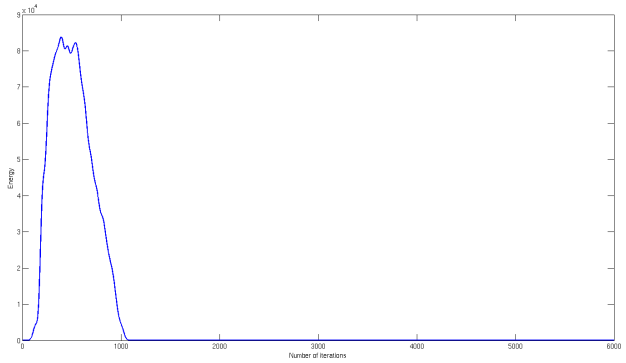

Figure 7: Decay of the energy: new condition.

Nevertheless we must observe that the experiments we have carried out concern the case of a circular boundary, for which the curvature ABC is already very accurate. Therefore we are now investigating the performances of the new ABC on an elliptic boundary. In particular, we wish to know if it can improve significantly the accuracy of the solution obtained with the C-ABC.

5 Conclusion

In this paper, we have proposed a new ABC for the acoustic wave equation that can be justify for any arbitrarily shaped surface by using a micro-local diagonalization process. This ABC has been written for all regular convex domains and both consider the hyperbolic and elliptic regions. We have performed some numerical tests in simple configurations and we have observed that the accuracy of the solution is improved. We plan to test numerically other configurations as elliptic domains or more general convex domains. We expect to see more significant improvements in the accuracy of the solution with such configurations than in the case of circular domains. We also plan to consider the case of the grazing modes that is to say when $\lambda_1 = 0$. In that case, the micro-local diagonalization process can not be applied but it might be possible to use an asymptotic expansion of the principal symbol of the acoustic wave equation [6].

A The IPDG method

In this appendix, we detail the construction of the IPDG method that we have used to test the ABCS.

We consider a partition $\mathcal{T}_h$ of Ω composed of triangles K, we denote by Ω_h the set of triangles, by Σ_{abs} the set of the edges on the absorbing boundary, by Σ_{N} the set of the edges on the Neumann boundary and by Σ_{i} the set of the edges in the domain such that $\Sigma_{\text{i}} \cap (\Sigma_{\text{N}} \cup \Sigma_{\text{abs}}) = \emptyset$. For each $\Sigma \in \Sigma_{\text{i}}$, we have to distinguish the two triangles that share Σ: we note them arbitrarily K^+ and K^-. We introduce useful notations to define the jump and the average over edges

$$[\![v]\!] := v^+ \boldsymbol{\nu}^+ + v^- \boldsymbol{\nu}^- \qquad \text{and} \qquad \{\{v\}\} := \frac{v^+ + v^-}{2},$$

where v^+ and v^- respectively refers to the restriction of v in K^+ and K^- and $\boldsymbol{\nu}^\pm$ stands for the unit outward normal vector to $K^\pm$.

It is well-known that the IPDG formulation of $(\mathcal{S})$ reads as [1, 11]

$$\begin{cases} \text{Find } u \in \mathcal{U} \text{ such that, } \forall v \in \mathrm{H}^1(\Omega), \\ \displaystyle\sum_{K \in \mathcal{T}_h} \int_K \partial_t^2 uv + a(u,v) - \sum_{\Sigma \in \Sigma_{\text{abs}}} \int_\Sigma c^2 \partial_{\mathbf{n}} uv = \sum_{K \in \mathcal{T}_h} \int_K fv \end{cases}$$

with

$$a(u,v) = \sum_K \int_K c^2 \nabla u \nabla v - \sum_{\Sigma \in \Sigma_{\text{i}}} \int_\Sigma \Big(\{\{c\nabla u\}\} [\![v]\!] + \{\{c\nabla v\}\} [\![u]\!] + \alpha [\![u]\!] [\![v]\!] \Big)$$

and α a penalization coefficient. We seek an approximation of the solution in the finite element space V_h^k defined as follows

$$V_h^k = \Big\{ v \in L^2(\Omega); v_{|K} \in P^k, \forall K \in \mathcal{T}_h \Big\}, \qquad k \in \mathbb{N},$$

where P^k is the set of polynomials of degree at most k on K.

The discrete problem is given by

$$(\mathcal{S}_h)\begin{cases}\text{Find } u_h\in V_h^k \text{ such that, } \forall v_h\in V_h^k,\\ \displaystyle\sum_{K\in\mathcal{T}_h}\int_K\frac{\partial^2 u_h}{\partial t^2}v_h-\sum_{\Sigma\in\Sigma_{\text{abs}}}c^2Bu_hv_h+a(u_h,v_h)=\sum_{K\in\mathcal{T}_h}\int_K fv_h.\end{cases}\tag{A.1}$$

For the sake of simplicity, we consider a well-known first-order ABC to explain its implementation in the IPDG formulation

$$\left(\partial_t+\partial_n+\frac{\kappa}{2}\right)u=0\quad\text{ on }\ \Gamma_{\text{abs}},\tag{A.2}$$

where κ is the curvature of Γ_{abs}.

In this case, we have

$$(\mathcal{S}_h)\begin{cases}\text{Find } u_h\in V_h^k \text{ such that, } \forall v_h\in V_h^k,\\ \displaystyle\sum_{K\in\mathcal{T}_h}\int_K\frac{\partial^2 u_h}{\partial t^2}v_h+a(u_h,v_h)+\sum_{\Sigma\in\Sigma_{\text{abs}}}c^2\int_\Sigma\left(\frac{\partial u_h}{\partial t}v_h+\frac{\kappa(.)}{2}u_hv_h\right)=\sum_{K\in\mathcal{T}_h}\int_K fv_h.\end{cases}\tag{A.3}$$

We already know that, to determine u_h on a given triangle we need C_{k+2}^k degrees of freedom. Since we consider a DG method we will have $N:=number of triangles\times C_{k+2}^k$ degrees of freedom in the whole domain. Let us consider $\{v_i,\,1\le i\le N\}$ a basis of V_h^k. We can rewrite u_h as $u_h(x,t)=\sum_{i=1}^N U_i(t)v_i(x)$.

The algebraic form of this problem is given by

$$M\frac{d^2\mathbf{U}}{dt^2}+B\frac{d\mathbf{U}}{dt}+B_\kappa\mathbf{U}+K\mathbf{U}=\mathbf{F},\tag{A.4}$$

where M is the mass matrix, K the stiffness matrix and

$$\begin{aligned}&\mathbf{U}=(U_i)_{1\le i\le N}, && M=\left(\sum_{K\in\mathcal{T}_h}\int_K v_iv_j\right)_{1\le i,j\le N},\\ &B=\left(\sum_{\Sigma\in\Sigma_{\text{abs}}}c^2\int_\Sigma v_iv_j\right)_{1\le i,j\le N}, && B_\kappa=\left(\sum_{\Sigma\in\Sigma_{\text{abs}}}\int_\Sigma\frac{\kappa}{2}v_iv_j\right)_{1\le i,j\le N},\\ &K=\left(a(v_i,v_j)\right)_{1\le i,j\le N}, && \mathbf{F}=\left(\sum_{K\in\mathcal{T}_h}\int_K fv_i\right)_{1\le i\le N}.\end{aligned}\tag{A.5}$$

As for the time discretization, we use a finite difference scheme of order two with a time step Δt and we obtain

$$\begin{aligned}&\left(M+\frac{\Delta t}{2}B+\frac{\Delta t^2}{2}B_\kappa\right)\mathbf{U}^{n+1}\\ &=\Delta t^2\mathbf{F}-\Delta t^2K\mathbf{U}^n+2M\mathbf{U}^n-M\mathbf{U}^{n-1}+\frac{\Delta t}{2}B\mathbf{U}^{n-1}-\frac{\Delta t^2}{2}B_\kappa\mathbf{U}^{n-1}.\end{aligned}\tag{A.6}$$

Remark A.1. We can remark that $(M+\frac{\Delta t}{2}B+\frac{\Delta t^2}{2}B_\kappa)$ is easily invertible because it is a block-diagonal matrix.

References

[1] M. Ainsworth, P. Monk, W. Muniz, Dispersive and dissipative properties of discontinuous Galerkin finite element methods for the second-order wave equation, J. Sci. Comput., 27(1-3) (2006), 5-40.

[2] X. Antoine, H. Barucq, Microlocal diagonalization of strictly hyperbolic pseudodifferential systems and application to the design of radiation conditions in electromagnetism, SIAM J. Appl. Math., 61 (2001), 1877-1905.

[3] X. Antoine, H. Barucq, A. Bendali, Bayliss-Turkel like radiation conditions on surfaces of arbitrary shape, J. Math. Anal. Appl., 229 (1999), 184-211.

[4] H. Barucq, A new family of first-order boundary conditions for the Maxwell system: Derivation, well-posedness and long-time behavior, J. Math. Pure Appl., 82 (2002), 67-88.

[5] A. Bayliss, M. Gunzburger, E. Turkel, Boundary conditions for the numerical solution of elliptic equations in exterior regions, SIAM J. Appl. Math., 42 (2002), 430-451.

[6] D. Bouche, F. Molinet, Méthodes asymptotiques en électromagnétisme, Springer-Verlag, 1994.

[7] L. Cagniard, Reflection and refraction of progressive seismic waves, McGraw-Hill, 1962.

[8] V. Dolean, M.J. Gander, L. Gerardo-Giorda, Optimized Schwarz methods for Maxwells equations, SIAM J. Sci. Comput., 31(3) (2009), 2193-2213.

[9] M. Ehrhardt, Absorbing boundary conditions for hyperbolic systems, Numer. Math. Theor. Meth. Appl., 3 (2010), 295-337.

[10] B. Engquist, A. Majda, Absorbing boundary conditions for the numerical simulation of waves, Math. Comp., 31 (1977), 629-651.

[11] M.J. Grote, A. Schneebeli, D. Schötzau, Discontinuous Galerkin finite element method for the wave equation, SIAM J. Numer. Anal., 44 (2006), 2408-2431.

[12] T. Hagstrom, D. Givoli, T. Warburton, Radiation boundary conditions for time-dependent waves based on complete plane wave expansions, J. Comput. Appl. Math., 234 (2010), pp. 1988-1995.

[13] T. Hagstrom, A. Mar-Or, D. Givoli, High-order local absorbing conditions for the wave equation: Extensions and improvements, J. Comput. Phys., 227 (2008), 3322-3357.

[14] T. Hagstrom, T. Warburton, Complete radiation boundary conditions: Minimizing the long time error growth of local methods, SIAM J. Numer. Anal., 47 (2009), pp. 3678-3704.

[15] R. Higdon, Numerical absorbing boundary conditions for the wave equation, Math. Comp., 49 (1987), 65-90.

[16] L. Hörmander, Pseudodifferential operators and hypoelliptic equations, in Proc. Sym. Pure Math. X (Singular Integrals), 138-183, AMS, Providence, 1967.

[17] R.C. Reiner, R. Djellouli, I. Harari, The performance of local absorbing boundary conditions for acoustic scattering from elliptical shapes, Comp. Meth. Appl. Mech. Engrg., 195 (2006), 3622-3665.

[18] M.E. Taylor, Pseudodifferential Operators, Princeton University Press, NJ, 1981.